Journal of Thermal Stresses
Publication details, including instructions for authors and subscription information:
http://www.informaworld.com/smpp/title~content=t713723680

Stress Analysis of a Penny-Shaped Crack in a Magneto-Electro-Thermo-Elastic Layer Under Uniform Heat Flow and Shear Loads

W. J. Feng [ab]; E. Pan [b]; X. Wang [b]
[a] Department of Engineering Mechanics, Shijiazhuang Railway Institute, Shijiazhuang, P.R. China
[b] Department of Civil Engineering, The University of Akron, Akron, OH, USA

Online Publication Date: 01 June 2008

To cite this Article: Feng, W. J., Pan, E. and Wang, X. (2008) 'Stress Analysis of a Penny-Shaped Crack in a Magneto-Electro-Thermo-Elastic Layer Under Uniform Heat Flow and Shear Loads', Journal of Thermal Stresses, 31:6, 497 — 514

To link to this article: DOI: 10.1080/01495730801912744
URL: http://dx.doi.org/10.1080/01495730801912744

Journal of Thermal Stresses, 31: 497–514, 2008

ISSN: 0149-5739 print/1521-074X online
DOI: 10.1080/01495730801912744

STRESS ANALYSIS OF A PENNY-SHAPED CRACK IN A MAGNETO-ELECTRO-THERMO-ELASTIC LAYER UNDER UNIFORM HEAT FLOW AND SHEAR LOADS

W. J. Feng[1,2], E. Pan[2], and X. Wang[2]
[1]*Department of Engineering Mechanics, Shijiazhuang Railway Institute, Shijiazhuang, P.R. China*
[2]*Department of Civil Engineering, The University of Akron, Akron, OH, USA*

This article analyzes the mechanical behavior induced by a penny-shaped crack in a magneto-electro-thermal-elastic layer that is subjected to a heat flow. The surfaces of the magneto-electro-thermal-elastic layer are subjected to radial shear loads, and the crack is assumed to be thermally insulated. The Hankel transform technique is employed to reduce the problem to a Fredholm integral equation, which is then solved numerically. Shear stress intensity factors (SIFs) are obtained and discussed in detail. Numerical results reveal that in the case of only applied shear loads, the layer height has insignificant effects on the SIF when the ratio of the half-layer height h to crack radius a is larger than 2, and that in the case of only applied heat flow, the layer height also has insignificant effects on the crack extension force when $h/a > 8$. It is further interesting to note that for the magneto-electro-thermo-elastic layer under only applied heat flow, there exists a critical height as far as the stability of the crack is concerned.

Keywords: Layer; Magneto-electro-elastic materials; Penny-shaped crack; Thermal stresses

INTRODUCTION

The magneto-electro-elastic materials are used to refer to a class of materials exhibiting full coupling between magnetic, electric and mechanical fields. Because of their remarkable magnetoelectric coupling effect, magneto-electro-elastic materials are potential candidates for use as magnetoelectric memory elements, smart sensors, and transducers, etc. However, a main disadvantage of magneto-electro-elastic materials is that they are very susceptible to fracture because of their brittleness. Thus, the mechanical behavior of magneto-electro-elastic materials with cracks plays an important role in the analysis and design of smart structures and devices.

In recent years, some investigations have been made on the fracture mechanics of anti-plane problems [1–8] and two-dimensional in-plane problems [9–17] of

Received 15 October 2007; accepted 3 January 2008.
Support from the Natural Science Fund of China (10772123) and AFOSR FA9550-06-1-0317 is acknowledged.
Address correspondence to W. J. Feng, Department of Engineering Mechanics, Shijiazhuang Railway Institute, Shijiazhuang, P.R. China. E-mail: wjfeng999@yahoo.com

magneto-electro-elastic materials. However, only few achievements are reported for penny-shaped crack problems because of their mathematical complexity. Among these limited literatures [18–21], Zhao et al. [18] derived the solution for an ellipsoidal cavity in an infinite transversely isotropic magneto-electro-elastic medium, and obtained the exact solution for a penny-shaped crack by letting the minor axis of the ellipsoidal cavity approach zero. Zhao et al. [19] analyzed the problem of planar crack of arbitrary shape in an isotropic plane of a three-dimensional transversely isotropic magnetoelectroelastic medium by using the hyper-singular integral equation method. Niraula and Wang [20] derived an exact closed-form solution for a penny-shaped crack in am infinite magneto-electro-thermo-elastic material in a temperature field, where the problem was transformed into dual integral equations which were solved directly. Wang and Niraula [21] further considered transient thermal fracture problem of transversely isotropic magneto-electro-elastic materials, where the problem is reduced into integral equation which is treated exactly using Abel's integral equation. To the best of our knowledge, these studies all considered a crack in an infinite magneto-electro-elastic body; to date, the penny-shaped crack problems under both mechanical load and thermal flow in the coupled magneto-electro-elastic materials have not been addressed yet, especially for a finite magneto-electro-elastic body.

In this article, the fracture properties of a penny-shaped crack embedded in a magneto-electro-elastic layer of finite height under both thermal flow and radial shear loads is investigated. Thermally insulated crack surface assumption is adopted. By means of the Hankel transform technique, the problem is finally reduced to solve a Fredholm integral equation, which is different to [18–21]. Stress intensity factors (SIFs) is obtained in a clear form. Numerical computations are carried out to evaluate the effects of the layer height on the SIFs.

STATEMENT OF THE PROBLEM

Basic Equations

Consider a class of axisymmetric problems of a transversely isotropic magneto-electro-thermo-elastic layer of height $2h$ with the poling direction as the z-axis and the isotropic plane as the xy-plane. The constitutive equations within the framework of the theory of linear magneto-electro-thermo-elastic medium can be given as [20]

$$\begin{Bmatrix} \sigma_{rr} \\ \sigma_{\theta\theta} \\ \sigma_{zz} \\ \sigma_{rz} \end{Bmatrix} = \begin{bmatrix} c_{11} & c_{12} & c_{13} & 0 \\ c_{12} & c_{11} & c_{13} & 0 \\ c_{13} & c_{13} & c_{33} & 0 \\ 0 & 0 & 0 & c_{44} \end{bmatrix} \begin{Bmatrix} \dfrac{\partial u_r}{\partial r} \\ \dfrac{u_r}{r} \\ \dfrac{\partial u_z}{\partial z} \\ \dfrac{\partial u_r}{\partial z} + \dfrac{\partial u_z}{\partial r} \end{Bmatrix} + \begin{bmatrix} 0 & e_{31} \\ 0 & e_{31} \\ 0 & e_{33} \\ e_{15} & 0 \end{bmatrix} \begin{Bmatrix} \dfrac{\partial \phi}{\partial r} \\ \dfrac{\partial \phi}{\partial z} \end{Bmatrix}$$

$$+\begin{bmatrix} 0 & f_{31} \\ 0 & f_{31} \\ 0 & f_{33} \\ f_{15} & 0 \end{bmatrix} \begin{Bmatrix} \dfrac{\partial \psi}{\partial r} \\ \dfrac{\partial \psi}{\partial z} \end{Bmatrix} - \begin{bmatrix} \lambda_{11} \\ \lambda_{11} \\ \lambda_{33} \\ 0 \end{bmatrix} T \tag{1a}$$

$$\begin{Bmatrix} D_r \\ D_z \end{Bmatrix} = \begin{bmatrix} 0 & 0 & 0 & e_{15} \\ e_{31} & e_{31} & e_{33} & 0 \end{bmatrix} \begin{Bmatrix} \dfrac{\partial u_r}{\partial r} \\ \dfrac{u_r}{r} \\ \dfrac{\partial u_z}{\partial z} \\ \dfrac{\partial u_r}{\partial z} + \dfrac{\partial u_z}{\partial r} \end{Bmatrix} - \begin{bmatrix} \varepsilon_{11} & 0 \\ 0 & \varepsilon_{33} \end{bmatrix} \begin{Bmatrix} \dfrac{\partial \phi}{\partial r} \\ \dfrac{\partial \phi}{\partial z} \end{Bmatrix}$$

$$- \begin{bmatrix} g_{11} & 0 \\ 0 & g_{33} \end{bmatrix} \begin{Bmatrix} \dfrac{\partial \psi}{\partial r} \\ \dfrac{\partial \psi}{\partial z} \end{Bmatrix} + \begin{Bmatrix} 0 \\ \tau_3 \end{Bmatrix} T \tag{1b}$$

$$\begin{Bmatrix} B_r \\ B_z \end{Bmatrix} = \begin{bmatrix} 0 & 0 & 0 & f_{15} \\ f_{31} & f_{31} & f_{33} & 0 \end{bmatrix} \begin{Bmatrix} \dfrac{\partial u_r}{\partial r} \\ \dfrac{u_r}{r} \\ \dfrac{\partial u_z}{\partial z} \\ \dfrac{\partial u_r}{\partial z} + \dfrac{\partial u_z}{\partial r} \end{Bmatrix} - \begin{bmatrix} g_{11} & 0 \\ 0 & g_{33} \end{bmatrix} \begin{Bmatrix} \dfrac{\partial \phi}{\partial r} \\ \dfrac{\partial \phi}{\partial z} \end{Bmatrix}$$

$$- \begin{bmatrix} \mu_{11} & 0 \\ 0 & \mu_{33} \end{bmatrix} \begin{Bmatrix} \dfrac{\partial \psi}{\partial r} \\ \dfrac{\partial \psi}{\partial z} \end{Bmatrix} + \begin{Bmatrix} 0 \\ \rho_3 \end{Bmatrix} T \tag{1c}$$

$$\begin{Bmatrix} q_r \\ q_z \end{Bmatrix} = - \begin{bmatrix} \kappa_{11} & 0 \\ 0 & \kappa_{33} \end{bmatrix} \begin{Bmatrix} \dfrac{\partial T}{\partial r} \\ \dfrac{\partial T}{\partial z} \end{Bmatrix} \tag{1d}$$

where corresponding components are functions of r and z, independent of angle θ. u_r and u_z are the radial and axial components of elastic displacements, respectively; ϕ and ψ are the electric and magnetic potentials, respectively; σ, D, B and q are the stress, electric displacement, magnetic induction and heat flow, respectively; c_{ij}, e_{ij}, f_{ij} and g_{ij} are the elastic, piezoelectric, piezomagnetic and magnetoelectric constants, respectively; ε_{ij} and μ_{ij} are the dielectric permittivities and magnetic permeabilities, respectively; κ_{ij} and λ_{ij} are the heat conduction coefficients and thermal stress constants, respectively; τ_3 and ρ_3 are the pyroelectric and pyromagnetic coefficients, respectively; T denotes temperature change. It should be pointed out that similar to D_r of piezoelectric ceramics [22], both B_r and D_r for magneto-electro-thermal-elastic

materials are assumed to be independent on temperature change T for the axisymmetric problems considered here. There are some differences with those for infinite magneto-electro-thermal-elastic body described in the early article [20].

In the absence of body forces, free charge density, free current density and thermal sources, stresses, electric displacements, magnetic inductions and thermal heat flows satisfy the following equilibrium equations:

$$\frac{\partial \sigma_{rr}}{\partial r} + \frac{\partial \sigma_{rz}}{\partial z} + \frac{\sigma_{rr} - \sigma_{\theta\theta}}{r} = 0 \tag{2a}$$

$$\frac{\partial \sigma_{rz}}{\partial r} + \frac{\partial \sigma_{zz}}{\partial z} + \frac{\sigma_{rz}}{r} = 0 \tag{2b}$$

$$\frac{\partial D_r}{\partial r} + \frac{\partial D_z}{\partial z} + \frac{D_r}{r} = 0 \tag{2c}$$

$$\frac{\partial B_r}{\partial r} + \frac{\partial B_z}{\partial z} + \frac{B_r}{r} = 0 \tag{2d}$$

$$\frac{\partial q_r}{\partial r} + \frac{\partial q_z}{\partial z} + \frac{q_r}{r} = 0 \tag{2e}$$

Substituting the constitutive equations into the above equations yields the basic governing equations for elastic displacements u_r and u_z, electric potential ϕ, and magnetic potential ψ as follows

$$c_{11}\left(\frac{\partial^2 u_r}{\partial r^2} + \frac{1}{r}\frac{\partial u_r}{\partial r} - \frac{u_r}{r^2}\right) + c_{44}\frac{\partial^2 u_r}{\partial z^2} + (c_{13} + c_{44})\frac{\partial^2 u_z}{\partial r \partial z} + (e_{31} + e_{15})\frac{\partial^2 \phi}{\partial r \partial z} + (f_{31} + f_{15})\frac{\partial^2 \psi}{\partial r \partial z} = \lambda_{11}\frac{\partial T}{\partial r} \tag{3a}$$

$$c_{44}\left(\frac{\partial^2 u_z}{\partial r^2} + \frac{1}{r}\frac{\partial u_z}{\partial r}\right) + c_{33}\frac{\partial^2 u_z}{\partial z^2} + (c_{13} + c_{44})\left(\frac{\partial^2 u_r}{\partial r \partial z} + \frac{1}{r}\frac{\partial u_r}{\partial z}\right) + e_{15}\left(\frac{\partial^2 \phi}{\partial r^2} + \frac{1}{r}\frac{\partial \phi}{\partial r}\right) + e_{33}\frac{\partial^2 \phi}{\partial z^2} + f_{15}\left(\frac{\partial^2 \psi}{\partial r^2} + \frac{1}{r}\frac{\partial \psi}{\partial r}\right) + f_{33}\frac{\partial^2 \psi}{\partial z^2} = \lambda_{33}\frac{\partial T}{\partial z} \tag{3b}$$

$$(e_{31} + e_{15})\left(\frac{\partial^2 u_r}{\partial r \partial z} + \frac{1}{r}\frac{\partial u_r}{\partial z}\right) + e_{15}\left(\frac{\partial^2 u_z}{\partial r^2} + \frac{1}{r}\frac{\partial u_z}{\partial r}\right) + e_{33}\frac{\partial^2 u_z}{\partial z^2} - \varepsilon_{11}\left(\frac{\partial^2 \phi}{\partial r^2} + \frac{1}{r}\frac{\partial \phi}{\partial r}\right) - \varepsilon_{33}\frac{\partial^2 \phi}{\partial z^2} - g_{11}\left(\frac{\partial^2 \psi}{\partial r^2} + \frac{1}{r}\frac{\partial \psi}{\partial r}\right) - g_{33}\frac{\partial^2 \psi}{\partial z^2} = -\tau_3\frac{\partial T}{\partial z} \tag{3c}$$

$$(f_{31} + f_{15})\left(\frac{\partial^2 u_r}{\partial r \partial z} + \frac{1}{r}\frac{\partial u_r}{\partial z}\right) + f_{15}\left(\frac{\partial^2 u_z}{\partial r^2} + \frac{1}{r}\frac{\partial u_z}{\partial r}\right) + f_{33}\frac{\partial^2 u_z}{\partial z^2} - g_{11}\left(\frac{\partial^2 \phi}{\partial r^2} + \frac{1}{r}\frac{\partial \phi}{\partial r}\right) - g_{33}\frac{\partial^2 \phi}{\partial z^2} - \mu_{11}\left(\frac{\partial^2 \psi}{\partial r^2} + \frac{1}{r}\frac{\partial \psi}{\partial r}\right) - \mu_{33}\frac{\partial^2 \psi}{\partial z^2} = -\rho_3\frac{\partial T}{\partial z} \tag{3d}$$

$$\kappa_{11}\left(\frac{\partial^2 T}{\partial r^2} + \frac{1}{r}\frac{\partial T}{\partial r}\right) + \kappa_{33}\frac{\partial^2 T}{\partial z^2} = 0 \tag{3e}$$

Boundary Conditions

As shown in Figure 1, a penny-shaped crack of radius a perpendicular to the poling axis is situated at the mid-plane of the layer and occupies the region $r \leq a$, $z = 0$. For magneto-electro-thermo-elastic body, lots of kinds of magnetoelectromechanical loads can be applied on the surfaces of the layer. The crack surface conditions for both magnetic and electric fields are also very complicated [16]. For the present mechanical model, we assume the surfaces of the layer to be subjected to only shear stress τ_0. Thus, because of the symmetry, from the view of fracture mechanics, the magnetoelectromechanical boundary condition in this case can equally be expressed as follows

$$\sigma_{zz}(r, \pm h) = 0, \quad \sigma_{zr}(r, \pm h) = 0 \;\; r < \infty \tag{4a}$$

$$D_z(r, \pm h) = 0, \quad B_z(r, \pm h) = 0 \;\; r < \infty \tag{4b}$$

for the top and lower surface, and

$$\sigma_{zz}(r, 0) = 0, \quad \sigma_{zr}(r, 0) = -\tau_0 \quad r < a \tag{5a}$$

$$D_z(r, 0) = 0, \quad B_z(r, 0) = 0 \quad r < a \tag{5b}$$

for the crack surfaces.

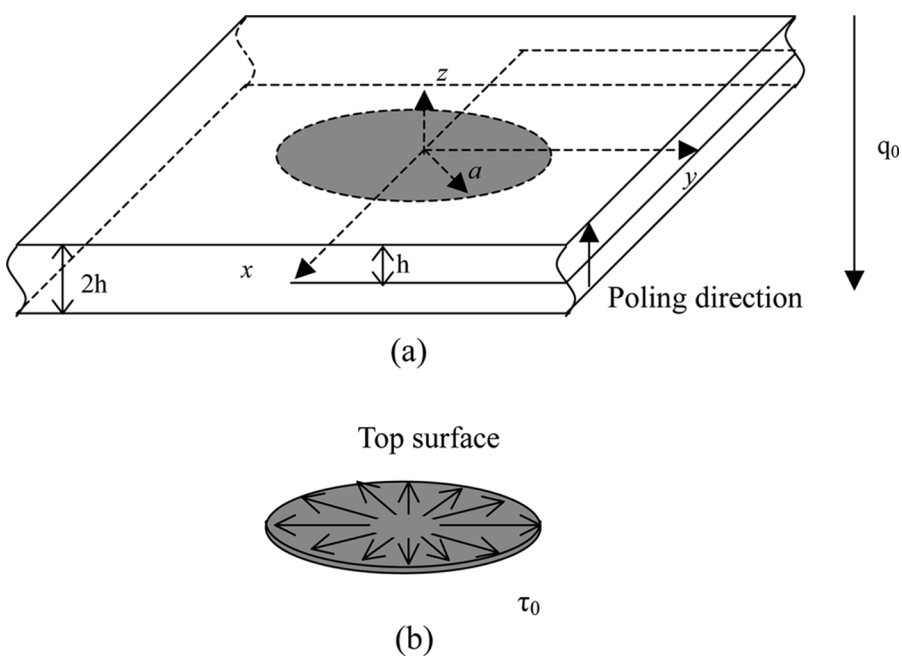

Figure 1 Magneto-electro-thermal-elastic layer with a horizontal, central, and penny-shaped crack subjected to heat flow and radial shear loads.

At the same time, assume the magneto-electro-thermal-elastic body to be subjected to uniform heat flow at the surface $z = h$ in the negative direction of the z-axis, and the crack is thermally insulated. Thus, the initial temperature field can be expressed as $T_0 = cz$, $c = -q_0/\kappa_{33}$, and the temperature field disturbed by the penny-shaped crack should satisfy the following boundary conditions [20]

$$T(r, \pm h) = 0, \quad r < \infty \tag{4c}$$

$$\frac{\partial T}{\partial z} = -c \quad r < a \;\; z = 0 \tag{5c}$$

Obviously, the problem considered here is anti-symmetric with respect to $z = 0$ plane simultaneously. Therefore, it is sufficient to consider only the upper half-space of the penny-shaped crack under the following additionally conditions:

$$\sigma_{zz}(r, 0) = 0, \quad u_r(r, 0) = 0 \quad a < r < \infty \tag{6a}$$

$$D_z(r, 0) = 0, \quad B_z(r, 0) = 0 \quad a < r < \infty \tag{6b}$$

$$T(r, 0) = 0 \quad a < r < \infty \tag{6c}$$

THE SOLUTION OF THERMAL FIELD

The thermal field is uncoupled with the magneto-electro-elastic field. Using the Hankel transform, the solution to the heat conduction equation (3e) can be expressed as follows

$$T(r, z) = \int_0^\infty [A_0(\xi)\sinh(\gamma_0\xi z) + B_0(\xi)\cosh(\gamma_0\xi z)]\, J_0(\xi r) d\xi \tag{7}$$

where $\gamma_0 = \sqrt{\kappa_{11}/\kappa_{33}}$, $J_0(\bullet)$ is a Bessel function of the first kind and zero order. Substituting Eq. (7) into Eq. (4c) yields

$$A_0(\xi) = -\coth(\gamma_0\xi h)\, B_0(\xi) \tag{8}$$

Substituting Eq. (7) into thermal conditions, i.e., Eqs. (5c) and (6c), a pair of dual integral equations about $B_0(\xi)$ is obtained as

$$\int_0^\infty \xi \coth(\gamma_0\xi h)\, B_0(\xi)\, J_0(\xi r) = c/\gamma_0 \quad r < a \tag{9a}$$

$$\int_0^\infty B_0(\xi)\, J_0(\xi r) = 0 \quad r > a \tag{9b}$$

The solution is [23]

$$B_0(\xi) = \frac{2ca^2}{\pi\gamma_0}\int_0^1 \Pi(t)\sin(\xi a t) dt \tag{10}$$

where $\Pi(t)$ satisfies the following Fredholm integral equation of the second kind:

$$\Pi(t) + \int_0^1 \Pi(\varsigma) K(t, \varsigma) d\varsigma = t \tag{11}$$

in which the kernel $K(t, \varsigma)$ is given as

$$K(t, \varsigma) = \frac{2}{\pi} \int_0^\infty [\coth(\gamma_0 sh/a) - 1] \sin(st) \sin(s\varsigma) ds \tag{12}$$

The Fredholm integral Eq. (11) can easily be solved numerically.

THE SOLUTION OF MAGNETO-ELECTRO-ELASTIC FIELD

Expressions of Field Quantities

According to the theory of partial differential equations, the solution to Eqs. (3a) to (3d) consists of two parts, the first is the homogeneous solution denoted by $\{u_{1r}\ u_{1z}\ \phi_1\ \psi_1\}^{\mathrm{T}}$ in which the temperature effect vanishes, the second is the particular solution denoted by $\{u_{2r}\ u_{2z}\ \phi_2\ \psi_2\}^{\mathrm{T}}$.

As usual, it is convenient to employ the Hankel transform technique to solve the problems. Firstly, for homogeneous solution, we introduce a potential functions by Hankel transform of the zeroth order

$$F(r, z) = -\int_0^\infty \frac{1}{\xi} A(\xi) \exp(\gamma \xi z) J_0(\xi r)\, d\xi, \quad z \geq 0 \tag{13}$$

and set

$$u_{1r}(r, z) = \frac{\partial F}{\partial r} \quad u_{1z}(r, z) = \eta_1 \frac{\partial F}{\partial z} \quad \phi_1(r, z) = \eta_2 \frac{\partial F}{\partial z} \quad \psi_1(r, z) = \eta_3 \frac{\partial F}{\partial z} \tag{14}$$

where A, γ and $\eta_i (i = 1, 2, 3)$ are, respectively, an unknown function and material constants to be determined. After substituting Eq. (14) together with (13) into Eqs. (3a) to (3d), we obtain the general expressions for elastic displacements, electric potential and magnetic potential in terms of unknown function A_j and B_j as follows:

$$u_{1r}(r, z) = \sum_{j=1}^{4} \int_0^\infty \left[A_j(\xi) \sinh\left(\gamma_j \xi z\right) + B_j(\xi) \cosh\left(\gamma_j \xi z\right)\right] J_1(\xi r) d\xi \tag{15a}$$

$$u_{1z}(r, z) = -\sum_{j=1}^{4} \eta_{1j} \gamma_j \int_0^\infty \left[A_j(\xi) \cosh\left(\gamma_j \xi z\right) + B_j(\xi) \sinh\left(\gamma_j \xi z\right)\right] J_0(\xi r) d\xi \tag{15b}$$

$$\phi_1(r, z) = -\sum_{j=1}^{4} \eta_{2j} \gamma_j \int_0^\infty \left[A_j(\xi) \cosh\left(\gamma_j \xi z\right) + B_j(\xi) \sinh\left(\gamma_j \xi z\right)\right] J_0(\xi r) d\xi \tag{15c}$$

$$* \ \psi_1(r, z) = -\sum_{j=1}^{4} \eta_{3j} \gamma_j \int_0^\infty \left[A_j(\xi) \cosh\left(\gamma_j \xi z\right) + B_j(\xi) \sinh\left(\gamma_j \xi z\right)\right] J_0(\xi r) d\xi \tag{15d}$$

where γ_j $(j = 1, 2, 3, 4)$ are chosen such that $\mathrm{Re}(\gamma_j)$ are larger than zero, which satisfy the following characteristic equation:

$$\det\left(\Xi_j\right) = 0 \quad j = 1, 2, 3, 4 \tag{16}$$

with

$$\Xi_j = \begin{bmatrix} c_{11} - c_{44}\gamma_j^2 & (c_{13} + c_{44})\,\gamma_j & (e_{31} + e_{15})\,\gamma_j & (f_{31} + f_{15})\,\gamma_j \\ (c_{13} + c_{44})\,\gamma_j & c_{33}\gamma_j^2 - c_{44} & e_{33}\gamma_j^2 - e_{15} & f_{33}\gamma_j^2 - f_{15} \\ (e_{31} + e_{15})\,\gamma_j & e_{33}\gamma_j^2 - e_{15} & \varepsilon_{11} - \varepsilon_{33}\gamma_j^2 & g_{11} - g_{33}\gamma_j^2 \\ (f_{31} + f_{15})\,\gamma_j & f_{33}\gamma_j^2 - f_{15} & g_{11} - g_{33}\gamma_j^2 & \mu_{11} - \mu_{33}\gamma_j^2 \end{bmatrix} \tag{17}$$

and η_{1j}, η_{2j} and η_{3j} satisfy the following equations:

$$\Xi_j \left\{1 \; -\eta_{1j}\gamma_j \; -\eta_{2j}\gamma_j \; -\eta_{3j}\gamma_j\right\}\}^{\mathrm{T}} = \mathbf{0} \tag{18}$$

Similarly, by introducing Hankel transform, the particular solution can be expressed as

$$u_{2r}(r, z) = \eta_0 \int_0^\infty \frac{1}{\xi} B_0(\xi)[\cosh(\gamma_0\xi z) - \coth(\gamma_0\xi h)\sinh(\gamma_0\xi z)]J_1\,(\xi r)\,d\xi \tag{19a}$$

$$u_{2z}(r, z) = -\eta_{10}\gamma_0\eta_0 \int_0^\infty \frac{1}{\xi} B_0\,(\xi)\,[\sinh\,(\gamma_0\xi z) - \coth\,(\gamma_0\xi h)\cosh\,(\gamma_0\xi z)]\,J_0\,(\xi r)\,d\xi \tag{19b}$$

$$\phi_2(r, z) = -\eta_{20}\gamma_0\eta_0 \int_0^\infty \frac{1}{\xi} B_0\,(\xi)\,[\sinh\,(\gamma_0\xi z) - \coth\,(\gamma_0\xi h)\cosh\,(\gamma_0\xi z)]\,J_0\,(\xi r)\,d\xi \tag{19c}$$

$$\psi_2(r, z) = -\eta_{30}\gamma_0\eta_0 \int_0^\infty \frac{1}{\xi} B_0\,(\xi)\,[\sinh\,(\gamma_0\xi z) - \coth\,(\gamma_0\xi h)\cosh\,(\gamma_0\xi z)]\,J_0\,(\xi r)\,d\xi \tag{19d}$$

where η_0, η_{10}, η_{20} and η_{30} are obtained as follows:

$$\left\{\eta_0 \quad -\eta_{10}\gamma_0\eta_0 \quad -\eta_{20}\gamma_0\eta_0 \quad -\eta_{30}\gamma_0\eta_0\right\}^{\mathrm{T}} = \Xi_0^{-1}\left\{\lambda_{11} \quad \lambda_{33}\gamma_0 \quad -\tau_3\gamma_0 \quad -\rho_3\gamma_0\right\}^{\mathrm{T}} \tag{20}$$

Thus, the complete solution to Eqs. (3a) to (3d) can be given by

$$u_r(r, z) = u_{1r}(r, z) + u_{2r}(r, z) \tag{21a}$$

$$u_z(r, z) = u_{1z}(r, z) + u_{2z}(r, z) \tag{21b}$$

$$\phi(r, z) = \phi_1(r, z) + \phi_2\,(r, z) \tag{21c}$$

$$\psi(r, z) = \psi_1(r, z) + \psi_2\,(r, z) \tag{21d}$$

From the constitutive equations, the expressions for stresses, electric displacement and magnetic induction in terms of the unknown functions A_j and B_j can easily be derived as

$$\sigma_{zz}(r,z) = -\sum_{j=1}^{4}\beta_{1j}\int_0^\infty \xi\left[A_j(\xi)\sinh\left(\gamma_j\xi z\right) + B_j(\xi)\cosh\left(\gamma_j\xi z\right)\right]J_0(\xi r)d\xi$$
$$-\left(\beta_{10}+\lambda_{33}\right)\eta_0\int_0^\infty B_0(\xi)\left[\cosh\left(\gamma_0\xi z\right) - \coth\left(\gamma_0\xi h\right)\sinh\left(\gamma_0\xi z\right)\right]J_0(\xi r)d\xi \tag{22a}$$

$$\sigma_{rz}(r,z) = \sum_{j=1}^{4}\beta_{2j}\int_0^\infty \xi\left[A_j(\xi)\cosh\left(\gamma_j\xi z\right) + B_j(\xi)\sinh\left(\gamma_j\xi z\right)\right]J_1(\xi r)d\xi$$
$$+\beta_{20}\eta_0\int_0^\infty B_0(\xi)\left[\sinh(\gamma_0\xi z) - \coth(\gamma_0\xi h)\cosh(\gamma_0\xi z)\right]J_1(\xi r)d\xi \tag{22b}$$

$$D_z(r,z) = -\sum_{j=1}^{4}\beta_{3j}\int_0^\infty \xi\left[A_j(\xi)\sinh\left(\gamma_j\xi z\right) + B_j(\xi)\cosh\left(\gamma_j\xi z\right)\right]J_0(\xi r)d\xi$$
$$-(\beta_{30}-\tau_3)\eta_0\int_0^\infty B_0(\xi)\left[\cosh(\gamma_0\xi z) - \coth(\gamma_0\xi h)\sinh(\gamma_0\xi z)\right]J_0(\xi r)d\xi \tag{22c}$$

$$B_z(r,z) = -\sum_{j=1}^{4}\beta_{4j}\int_0^\infty \xi\left[A_j(\xi)\sinh\left(\gamma_j\xi z\right) + B_j(\xi)\cosh\left(\gamma_j\xi z\right)\right]J_0(\xi r)d\xi$$
$$-(\beta_{40}-\rho_3)\eta_0\int_0^\infty B_0(\xi)\left[\cosh(\gamma_0\xi z) - \coth(\gamma_0\xi h)\sinh(\gamma_0\xi z)\right]J_0(\xi r)d\xi \tag{22d}$$

where

$$\beta_{1j} = \left(c_{33}\eta_{1j} + e_{33}\eta_{2j} + f_{33}\eta_{3j}\right)\gamma_j^2 - c_{13} \quad j = 1,2,3,4,0 \tag{23a}$$
$$\beta_{2j} = \left[c_{44}\left(1+\eta_{1j}\right) + e_{15}\eta_{2j} + f_{15}\eta_{3j}\right]\gamma_j \quad j = 1,2,3,4,0 \tag{23b}$$
$$\beta_{3j} = \left(e_{33}\eta_{1j} - \varepsilon_{33}\eta_{2j} - g_{33}\eta_{3j}\right)\gamma_j^2 - e_{31} \quad j = 1,2,3,4,0 \tag{23c}$$
$$\beta_{4j} = \left(f_{33}\eta_{1j} - g_{33}\eta_{2j} - \mu_{33}\eta_{3j}\right)\gamma_j^2 - f_{31} \quad j = 1,2,3,4,0 \tag{23d}$$

Solution and Derivation of Dual Integral Equations

From Eq. (22) and the boundary conditions (4a) and (4b), we have

$$\mathbf{A} = \mathbf{Z}_a^{-1}\left(\frac{1}{\xi}\eta_0 B_0(\xi)\,\mathbf{R} - \mathbf{Z}_b\mathbf{B}\right) \tag{24}$$

where

$$\mathbf{A} = \begin{Bmatrix} A_1(\xi) \\ A_2(\xi) \\ A_3(\xi) \\ A_4(\xi) \end{Bmatrix} \quad \mathbf{B} = \begin{Bmatrix} B_1(\xi) \\ B_2(\xi) \\ B_3(\xi) \\ B_4(\xi) \end{Bmatrix} \quad \mathbf{R} = \begin{Bmatrix} 0 \\ \beta_{20}\mathrm{csch}(\gamma_0\xi h) \\ 0 \\ 0 \end{Bmatrix} \tag{25a}$$

$$\mathbf{Z}_a = \begin{bmatrix} \beta_{11}\mathrm{sh}(\gamma_1\xi h) & \beta_{12}\mathrm{sh}(\gamma_2\xi h) & \beta_{13}\mathrm{sh}(\gamma_3\xi h) & \beta_{14}\mathrm{sh}(\gamma_4\xi h) \\ \beta_{21}\mathrm{ch}(\gamma_1\xi h) & \beta_{22}\mathrm{ch}(\gamma_2\xi h) & \beta_{23}\mathrm{ch}(\gamma_3\xi h) & \beta_{24}\mathrm{ch}(\gamma_4\xi h) \\ \beta_{31}\mathrm{sh}(\gamma_1\xi h) & \beta_{32}\mathrm{sh}(\gamma_2\xi h) & \beta_{33}\mathrm{sh}(\gamma_3\xi h) & \beta_{34}\mathrm{sh}(\gamma_4\xi h) \\ \beta_{41}\mathrm{sh}(\gamma_1\xi h) & \beta_{42}\mathrm{sh}(\gamma_2\xi h) & \beta_{43}\mathrm{sh}(\gamma_3\xi h) & \beta_{44}\mathrm{sh}(\gamma_4\xi h) \end{bmatrix} \tag{25b}$$

$$\mathbf{Z}_b = \begin{bmatrix} \beta_{11}\mathrm{ch}(\gamma_1\xi h) & \beta_{12}\mathrm{ch}(\gamma_2\xi h) & \beta_{13}\mathrm{ch}(\gamma_3\xi h) & \beta_{14}\mathrm{ch}(\gamma_4\xi h) \\ \beta_{21}\mathrm{sh}(\gamma_1\xi h) & \beta_{22}\mathrm{sh}(\gamma_2\xi h) & \beta_{23}\mathrm{sh}(\gamma_3\xi h) & \beta_{24}\mathrm{sh}(\gamma_4\xi h) \\ \beta_{31}\mathrm{ch}(\gamma_1\xi h) & \beta_{32}\mathrm{ch}(\gamma_2\xi h) & \beta_{33}\mathrm{ch}(\gamma_3\xi h) & \beta_{34}\mathrm{ch}(\gamma_4\xi h) \\ \beta_{41}\mathrm{ch}(\gamma_1\xi h) & \beta_{42}\mathrm{ch}(\gamma_2\xi h) & \beta_{43}\mathrm{ch}(\gamma_3\xi h) & \beta_{44}\mathrm{ch}(\gamma_4\xi h) \end{bmatrix} \tag{25c}$$

To determine unknown functions $\mathbf{B}(\xi)$, i.e., $B_j(\xi)$ $(j = 1, 2, 3, 4)$, a new auxiliary function $\overline{B}(\xi)$ is introduced as

$$\sum_{j=1}^{4} B_j(\xi) + \frac{1}{\xi}\eta_0 B_0(\xi) = \overline{B}(\xi) \tag{26a}$$

Substituting Eqs. (22a), (22c) and (22d) into Eqs. ($5a_1$), ($6a_1$), (5b) and (6b), i.e., $\sigma_{zz}(r, 0) = D_z(r, 0) = B_z(r, 0) = 0$, we can further obtain

$$\sum_{j=1}^{4} \beta_{1j} B_j(\xi) = -\frac{1}{\xi}(\beta_{10} + \lambda_{33})\eta_0 B_0(\xi) \tag{26b}$$

$$\sum_{j=1}^{4} \beta_{3j} B_j(\xi) = -\frac{1}{\xi}(\beta_{30} - \tau_3)\eta_0 B_0(\xi) \tag{26c}$$

$$\sum_{j=1}^{4} \beta_{4j} B_j(\xi) = -\frac{1}{\xi}(\beta_{40} - \rho_3)\eta_0 B_0(\xi) \tag{26d}$$

The unknown functions $B_j(\xi)$ $(j = 1, 2, 3, 4)$ can be given in terms of $\overline{B}(\xi)$ as

$$\mathbf{B}(\xi) = \mathbf{P}_a \overline{B}(\xi) - \frac{1}{\xi}\mathbf{P}_b \eta_0 B_0(\xi) \tag{27}$$

where

$$\mathbf{P}_a = \begin{bmatrix} \beta_{11} & \beta_{12} & \beta_{13} & \beta_{14} \\ 1 & 1 & 1 & 1 \\ \beta_{31} & \beta_{32} & \beta_{33} & \beta_{34} \\ \beta_{41} & \beta_{42} & \beta_{43} & \beta_{44} \end{bmatrix}^{-1} \begin{Bmatrix} 0 \\ 1 \\ 0 \\ 0 \end{Bmatrix} \quad \mathbf{P}_b = \begin{bmatrix} \beta_{11} & \beta_{12} & \beta_{13} & \beta_{14} \\ 1 & 1 & 1 & 1 \\ \beta_{31} & \beta_{32} & \beta_{33} & \beta_{34} \\ \beta_{41} & \beta_{42} & \beta_{43} & \beta_{44} \end{bmatrix}^{-1} \begin{Bmatrix} \beta_{10} + \lambda_{33} \\ 1 \\ \beta_{30} - \tau_3 \\ \beta_{40} - \rho_3 \end{Bmatrix} \tag{28}$$

Inserting Eqs. (21a), (26a) together with Eqs. (19a) and (15a) into the second equation of Eq. (6a) yields

$$\int_0^\infty \overline{B}(\xi) J_1(\xi r) = 0 \quad r > a \tag{29}$$

Substituting Eq. (27) into Eq. (24) yields

$$\mathbf{A} = -\mathbf{Z}_a^{-1}(\xi)\mathbf{Z}_b(\xi)\mathbf{P}_a\overline{B}(\xi) + \frac{1}{\xi}\eta_0 B_0(\xi)\left(\mathbf{Z}_a^{-1}(\xi)\mathbf{R}(\xi) + \mathbf{Z}_a^{-1}(\xi)\mathbf{Z}_b(\xi)\mathbf{P}_b\right) \tag{30}$$

Setting

$$\boldsymbol{\beta}_2 = \{\beta_{21} \quad \beta_{22} \quad \beta_{23} \quad \beta_{24}\} \tag{31}$$

it is known from Eq. (22b), that the only non-zero shear stress σ_{rz} on the crack plane can be expressed as

$$\begin{aligned} \sigma_{rz}(r,0) = &-\int_0^\infty w_1 \xi \overline{B}(\xi) J_1(\xi r) d\xi \\ &+ \int_0^\infty [w_2 - \beta_{20}\coth(\gamma_0 \xi h)]\eta_0 B_0(\xi) J_1(\xi r) d\xi \end{aligned} \tag{32}$$

where

$$w_1 = \boldsymbol{\beta}_2 \mathbf{Z}_a^{-1}(\xi)\mathbf{Z}_b(\xi)\mathbf{P}_a \quad w_2 = \boldsymbol{\beta}_2\left(\mathbf{Z}_a^{-1}(\xi)\mathbf{R}(\xi) + \mathbf{Z}_a^{-1}(\xi)\mathbf{Z}_b(\xi)\mathbf{P}_b\right) \tag{33}$$

Making use of Eq. ($5a_2$), we have

$$\int_0^\infty \xi G(\xi)\overline{B}(\xi) J_1(\xi r) d\xi = (\boldsymbol{\beta}_2\mathbf{P}_a)^{-1}\tau_0 + (\boldsymbol{\beta}_2\mathbf{P}_a)^{-1}\int_0^\infty f(\xi) J_1(\xi r) d\xi \quad r < a \tag{34}$$

where

$$G = (\boldsymbol{\beta}_2\mathbf{P}_a)^{-1}\boldsymbol{\beta}_2\mathbf{Z}_a^{-1}(\xi)\mathbf{Z}_b(\xi)\mathbf{P}_a \quad f(\xi) = [w_2 - \beta_{20}\coth(\gamma_0\xi h)]\eta_0 B_0(\xi) \tag{35}$$

As before, the solution to a pair of dual integral Eqs. (29) and (34) can be solved to render [23]

$$\overline{B}(\xi) = \sqrt{\pi/8}\, a^{5/2}(\boldsymbol{\beta}_2\mathbf{P}_a)^{-1}\sqrt{\xi}\int_0^1 \sqrt{t}\Delta(t) J_{3/2}(\xi a t) dt \tag{36}$$

where $\Delta(t)$ obeys the following Fredholm integral equation

$$\Delta(t) + \int_0^1 \Delta(\varsigma) Q(t, \varsigma)\, d\varsigma = \tau_0 t + (a\sqrt{\pi/8})^{-1}\sqrt{t}\int_0^\infty f\left(\frac{\varsigma}{a}\right)\varsigma^{-1/2} J_{3/2}(\varsigma t)\, d\varsigma \tag{37}$$

whose kernel $Q(t, \varsigma)$ takes the form

$$Q(t, \varsigma) = \sqrt{t\varsigma}\int_0^\infty s\left[G\left(\frac{s}{a}\right) - 1\right] J_{3/2}(st) J_{3/2}(s\varsigma) ds \tag{38}$$

The Fredholm integral Eq. (38) can easily be solved numerically. Up till now, all the unknown functions have been completely solved.

STRESS INTENSITY FACTORS

Integrations of $\overline{B}$ in Eq. (36) and B_0 in Eq. (10) by parts respectively give

$$\overline{B}(\xi) = \sqrt{\pi/8} a^{3/2} (\boldsymbol{\beta}_2 \mathbf{P}_a)^{-1} \xi^{-1/2}\left[-\Lambda(1) J_{1/2}(\xi a) + \int_0^1 s^{-1/2} J_{1/2}(\xi a s) \frac{d}{ds}(s\Lambda(s))\, ds\right] \tag{39a}$$

$$B_0(\xi) = \frac{2ca^2}{\pi\gamma_0}\left[\frac{1}{\xi a}\Pi(0) - \frac{\cos(\xi a)}{\xi a}\Pi(1) + \int_0^1 \frac{\cos(\xi a s)}{\xi a}\frac{d}{ds}(\Lambda(s))\, ds\right] \tag{39b}$$

Thus, the stress $\sigma_{rz}(r, 0)$ can be rewritten as

$$\sigma_{rz}(r, 0) = \frac{a}{2}(\boldsymbol{\beta}_2 \mathbf{P}_a)^{-1}\Delta(1)\int_0^\infty w_1 \sin(\xi a) J_1(\xi r)\, d\xi + \frac{2ca}{\pi\gamma_0}\int_0^\infty [w_2 - \beta_{20}\coth(\gamma_0 \xi h)] \times \eta_0([\Pi(0) - \cos(\xi a)\Pi(1)])\, \xi^{-1} J_1(\xi r)\, d\xi + \cdots \tag{40}$$

Because the integrands are finite and continuous for any given values of ξ, the divergence of the integrals at the crack frontier must be due to behavior as $\xi \to \infty$. Noting that

$$\lim_{\xi\to\infty} w_1 = \boldsymbol{\beta}_2 \mathbf{P}_a, \quad \lim_{\xi\to\infty}[w_2 - \beta_{20}\coth(\gamma_0 \xi h)] = \boldsymbol{\beta}_2 \mathbf{P}_b - \beta_{20} \tag{41}$$

carrying out the expansion for large ξ, we can easily obtain the lower-order singular term of the stress $\sigma_{rz}(r, 0)$ as follows

$$\sigma_{rz}(r, 0) \to \frac{a}{2}\Delta(1)\int_0^\infty \sin(\xi a) J_1(\xi r)\, d\xi \tag{42}$$

Using the known identity

$$\int_0^\infty \sin(\xi a) J_v(\xi r)\, d\xi = \sin\left(v \sin^{-1}\frac{a}{r}\right)\left(r^2 - a^2\right)^{-1/2} \quad r > a, \tag{43}$$

Eq. (42) can be expressed as

$$\sigma_{rz}(r,0) = \frac{\mathrm{K}_2}{\sqrt{2\pi(r-a)}} \tag{44}$$

where K_2 is the shear stress intensity factor (SIF), which is defined as

$$\mathrm{K}_2 = \lim_{z\to a^+} \sqrt{2(z-a)}\sigma_{zr}(r,0) \tag{45}$$

and given as

$$\mathrm{K}_2 = \frac{\sqrt{\pi a}}{2}\Delta(1) \tag{46}$$

where $\Delta(1)$ can be solved from Eq. (37) numerically. We remark that from Eqs. (46) and (37), it is easily seen that the stress intensity factor consists of two parts, the first is the one induced by the purely shear load, the second is the one corresponding to the heat flow.

FURTHER ANALYSIS ON THE SIF OF INFINITE MAGNETO-ELECTRO-THERMO-ELASTIC BODY

It is easily found that the resulting equations become very simple for a special case of $h \to \infty$. From Eq. (33), we obtain

$$\lim_{h\to\infty} w_1(\xi) \equiv \boldsymbol{\beta}_2\mathbf{P}_a \quad \lim_{h\to\infty} w_2(\xi) \equiv \boldsymbol{\beta}_2\mathbf{P}_b \tag{47}$$

Equation (47) implies that for infinite magneto-electro-thermal-elastic body, both w_1 and w_2 are independent of ξ. Thus, $G \equiv 1$, and Eq. (37) can then be transformed into as follows:

$$\Delta(t) = \tau_0 t + \left(a\sqrt{\pi/8}\right)^{-1}\sqrt{t}\int_0^\infty f\left(\frac{\varsigma}{a}\right)\varsigma^{-1/2}J_{3/2}(\varsigma t)\,d\varsigma \tag{48}$$

At the same time, from Eq. (12), we have $\lim_{h\to\infty} K(t,\varsigma) \equiv 0$, which yields from Eq. (10),

$$B_0(\xi) = \sqrt{2\pi^{-1}}ca^{3/2}\gamma_0^{-1}\xi^{-1/2}J_{3/2}(\xi a) \tag{49}$$

From Eqs. (35), (47) and (49), function $f(\xi)$ can also be given as

$$\lim_{h\to\infty} f(\xi) = \sqrt{2\pi^{-1}}\left(\boldsymbol{\beta}_2\mathbf{P}_b - \beta_{20}\right)\eta_0 ca^2\gamma_0^{-1}(\xi a)^{-1/2}J_{3/2}(\xi a) \tag{50}$$

Substituting Eq. (50) into Eq. (48), we finally obtain

$$\Delta(t) = \tau_0 t + \frac{4}{\pi}\left(\boldsymbol{\beta}_2\mathbf{P}_b - \boldsymbol{\beta}_{20}\right)\eta_0 a\sqrt{t}\int_0^\infty \zeta^{-1}J_{3/2}(\zeta)\,J_{3/2}(\zeta t)\,d\varsigma \tag{51}$$

By integrating Eq. (51) and substituting the obtained results into Eq. (34), we can rewriting the shear SIF as

$$\mathrm{K}_2 = \mathrm{K}_{0\tau} + \mathrm{K}_{0q} \tag{52}$$

where

$$\mathrm{K}_{0\tau} = \frac{\sqrt{\pi a}}{2}\tau_0 \tag{53}$$

$$\mathrm{K}_{0q} = \frac{2c}{3\sqrt{\pi}\gamma_0} a^{3/2}\eta_0 \left(\boldsymbol{\beta}_2 \mathbf{P}_b - \boldsymbol{\beta}_{20}\right) \tag{54}$$

Equations (52) to (54) indicate that for infinite magneto-electro-thermo-elastic medium, the SIF induced by purely shear loads (i.e., $k_{0\tau}$) is independent of material properties, which is quite in agreement with the one of a penny-shaped crack in an unbounded elastic material [23]. However, the SIF induced by heat flow (i.e., k_{0q}) depends on both the heat flow $q = -\kappa_{33}c$ and the material properties. Comparing Eq. (54) above with Eq. (49) in [20], it is found that they are almost the same except a coefficient 2. Maybe Eq. (49) in [20] has a minor printed error.

NUMERICAL EXAMPLES

In this section, some examples are further considered to evaluate the effects of layer height on the stress intensity factors under only shear load and/or heat flow. The magneto-electro-thermal-elastic body is taken as $BaTiO_3$-$CoFe_2O_4$ composite. The heat conduction coefficients, thermal stress constants, pyroelectric and pyromagnetic coefficients of the composite are given in Table 1, and the other material properties are taken from [16]. Numerical results under only shear load and/or heat flow are respectively plotted in Figures 2–3, where the SIFs are normalized by the corresponding SIFs of infinite magneto-electro-thermal-elastic materials (see Eqs. (53) and (54)), respectively.

Figure 2 shows that with the increasing of the layer height, the SIF decreases. However, as $h/a > 2$, the SIF rapidly tends to one (corresponding to infinite body), which implies, in a certain extent, that our formulations are reliable. It should be noted that for a penny-shaped crack in a magneto-electro-thermo-elastic layer under only shear load, as h/a goes to zero, the stress intensity factor, as expected, becomes unbounded.

Figure 3 shows that under only heat flow, the layer height has different effects on the crack extension force for the magneto-electro-thermal-elastic material considered here. As the layer is thinner, the SIF is less than zero. The critical value is about $h/a = 3.0$. That is to say, as the radio of the layer height to crack radius is

Table 1 Material properties

λ_{11} (N/Km^2)	λ_{33} (N/Km^2)	τ_3 (C/Km^2)	ρ_3 (N/KAm)	κ_{11} (W/mK)	κ_{33} (W/mK)
5.5271×10^6	4.958×10^6	-1.972×10^{-5}	-0.010328	50	75

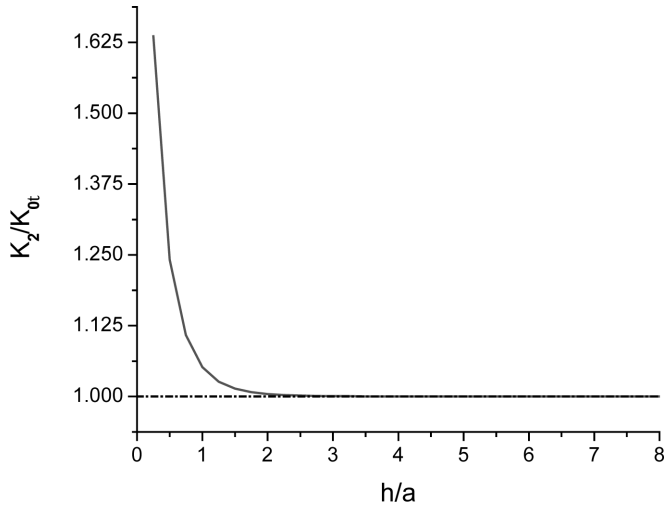

Figure 2 Normalized stress intensity factor K_2 as a function of h/a under shear loads only.

equal to 3.0, the crack is perhaps the most stable. As $h/a < 3.0$, the thinner the layer, the easier the crack propagation and growth is. However, as the height is larger than the critical value, the SIF increases with the increasing of h/a, which implies that increasing the layer height also enhances crack growth. It is pointed out that at this time, the direction of crack extension is different to the one corresponding to $h/a < 3.0$.

Similar phenomena have been observed for the problem of uniform heat flow disturbed by an inclined crack in an orthotropic rectangular plate (see pp. 1066 [24])

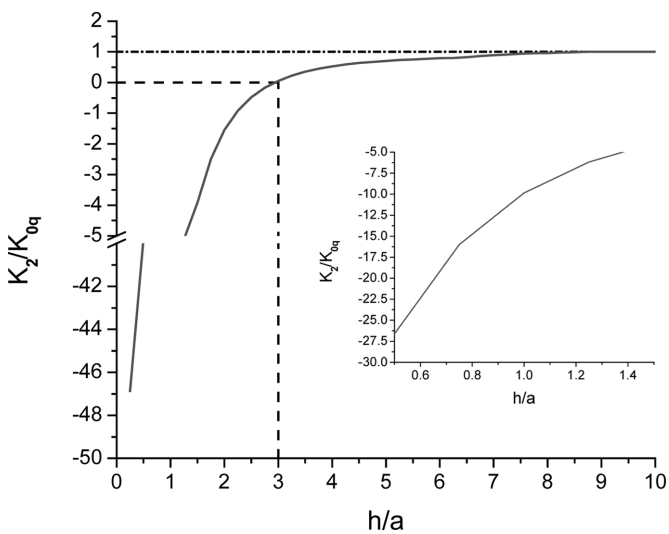

Figure 3 Normalized stress intensity factor K_2 as a function of h/a under thermal flow only.

and for the inclined crack problem of heated orthotropic rectangular plate (see pp. 1060 [24]). (By the way, for an inclined crack at a square notch in a semi-infinite plane under uniform tension, the phenomenon of changing sign of the mode II stress intensity factor also occurs for a certain crack configuration (see pp. 134 [24]).

Figure 3 also indicates that as $h/a > 8.0$, the SIF tends to one as well (corresponding to infinite body under only heat flow), which indicates that, similar to only applied shear load, when the height is larger than a definite value, further increasing layer height has also insignificant effects on the crack extension. However, it should be pointed out that, different to the applied shear load, with the increasing of h/a, the mode II stress intensity factor tends to the corresponding value of infinite magneto-electro-thermo-elastic body in a monotonically increasing trend under only thermal load. This trend is similar to the one for the problems of uniform heat flow on a penny-shaped crack parallel to free surface or rigidly clamped surface as the distance between the crack and the surface goes to infinity (see pp. 1087 [24]).

CONCLUSIONS

The stress of a penny-shaped crack in a magneto-electro-thermal-elastic layer subjected to heat flow and radial shear loads is investigated. For the present mechanical model, from the analysis and numerical results, the following conclusions can be drawn:

(1) The shear stress intensity factor of mode II is independent of magneto-electrical permeability of crack.

(2) The shear stress intensity factor consists of two parts, which are induced by shear loads and heart flow, respectively. For applied shear loads only, increasing the layer height can inhabit crack propagation. However, when the ratio of layer height to crack radius is larger than 2, increasing layer height has no obvious effects on the crack propagation and growth. For applied heat flow only, there exists a critical height. When the layer height is larger or less than the value, either increasing or decreasing the layer height can enhance crack propagation and growth towards different directions. In addition, for the material properties considered here, if the ratio of the layer height to crack radius is larger than 8, then increasing layer height has also insignificant effects on the crack extension.

(3) For the finite magneto-electro-thermal-elastic body, the stress intensity factor is related to material properties and layer height. However, for a crack in an infinite material under radial shear loads only, the stress intensity factor depends only on the applied shear load and crack size. Also, if the infinite magneto-electro-thermal-elastic material is subjected to only heat flow, the resulting thermal stress intensity factor is related to all of the material properties, the thermal load and the crack configuration.

REFERENCES

1. Z. G. Zhou, B. Wang, and Y. G. Sun, Two Collinear Interface Cracks in Magneto-Electro-Elastic Composites, *Int. J. Eng. Sci.*, vol. 42, pp. 1155–1167, 2004.

2. C. H. Chue and T. J. C. Liu, Magneto-Electro-Elastic Antiplane Analysis of a Biomaterial $BatiO_3$-$CoFe_2O_4$ Composite Wedge with an Interface Crack, *Theor. Appl. Fract. Mech.*, vol. 44, pp. 275–296, 2005.
3. W. J. Feng, Y. Xue, and Z. Z. Zou, Crack Growth of an Interface Crack Between Two Dissimilar Magneto-Electro-Elastic Materials under Anti-Plane Mechanical and In-Plane Electric Magnetic Impact, *Theor. Appl. Fract. Mech.*, vol. 43, pp. 376–394, 2005.
4. K. Q. Hu and G. Q. Li, Constant Moving Crack in a Magnetoelectroelastic Material under Anti-Plane Shear Loading, *Int. J. Solids Struct.*, vol. 42, pp. 2823–2835, 2005.
5. R. Li and G. A. Kardomateas, The Mode III Interface Crack in Piezo-Electro-Magneto-Elastic Dissimilar Bimaterials, *J. Appl. Mech.*, vol. 73, pp. 220–227, 2006.
6. B. L. Wang and Y. W. Mai, Closed-Form Solution for an Antiplane Interface Crack Between Two Dissimilar Magnetoelectroelastic Layers, *J. Appl. Mech.*, vol. 73, pp. 281–290, 2006.
7. W. J. Feng and R. K. L. Su, Dynamic Internal Crack Problem of a Functionally Graded Magneto-Electro-Elastic Strip, *Int. J. Solids Struct.*, vol. 43, pp. 5196–5216, 2006.
8. X. C. Zhong and X. F. Li, A Finite Length Crack Propagating along the Interface of Two Dissimilar Magnetoelectroelastic Materials, *Int. J. Eng. Sci.*, vol. 44, pp. 1394–1407, 2006.
9. Z. F. Song and G. C. Sih, Crack Initiation Behavior in Magnetoelectroelastic Composite under In-Plane Deformation, *Theor. Appl. Fract. Mech.*, vol. 39, pp. 189–207, 2003.
10. C. F. Gao, H. Kessler, and H. Balke, Crack Problems in Magnetoelectroelastic Solids. Part I: Exact Solution of a Crack, *Int. J. Eng. Sci.*, vol. 41, pp. 969–981, 2003.
11. C. F. Gao, H. Kessler, and H. Balke, Crack Problems in Magnetoelectroelastic Solids. Part II: General Solution of Collinear Cracks, *Int. J. Eng. Sci.*, vol. 41, pp. 983–994, 2003.
12. C. F. Gao, P. Tong, and T. Y. Zhang, Interfacial Crack Problems in Magneto-Electroelastic Solids, *Int. J. Eng. Sci.*, vol. 41, pp. 2105–2121, 2003.
13. W. Y. Tian and U. Gabbert, Multiple Crack Interaction Problem in Magnetoelectroelastic Solids, *Eur. J. Mech. A/Solids*, vol. 23, pp. 599–614, 2004.
14. G. C. Sih and H. Y. Yu, Volume Fraction Effect of Magnetoelectroelastic Composite on Enhancement and Impediment of Crack Growth, *Comp. Struct.*, vol. 68, pp. 1–11, 2005.
15. W. Y. Tina and U. Gabbert, Macrocrack-Microcrack Interaction Problem in Magnetoelectroelastic Solids, *Mech. Mater.*, vol. 37, pp. 565–592, 2005.
16. B. L. Wang and Y. W. Mai, Applicability of the Crack-Face Electromagnetic Boundary Conditions for Fracture of Magnetoelectroelastic Materials, *Int. J. Solids Struct.*, vol. 44, pp. 387–398, 2007.
17. P. W. Zhang, Z. G. Zhou, and L. Z. Wu, Solutions to Two or Four Parallel Mode-I Permeable Cracks in Magnetoelectroelastic Composite Materials, *Philosophical Magazine*, vol. 87, pp. 3175–3208, 2007.
18. M. H. Zhao, F. Yang, and T. Liu, Analysis of a Penny-Shaped Crack in a Magneto-Electro-Elastic Medium, *Philosophical Magazine*, vol. 86, pp. 4397–4416, 2006.
19. M. H. Zhao, C. Y. Fan, F. Yang, and T. Liu, Analysis Method of Planar Cracks of Arbitrary Shape in the Isotropic Plane of a Three-Dimensional Transversely Isotropic Magnetoelectroelastic Medium, *Int. J. Solids Struct.*, vol. 44, pp. 4505–4523, 2007.
20. O. P. Niraula and B. L. Wang, Thermal Stress Analysis in Magneto-Electro-Thermo-Elasticity with a Penny-Shaped Crack under Uniform Heat Flow, *J. Thermal Stresses*, vol. 29, pp. 423–437, 2006.
21. B. L. Wang and O. P. Niraula, Transient Thermal Fracture Analysis of Transversely Isotropic Magneto-Electro-Elastic Materials, *J. Thermal Stresses*, vol. 30, pp. 297–317, 2007.

22. S. Ueda, A Penny-Shaped Crack in a Functionally Graded Piezoelectric Strip under Thermal Loading, *Eng. Fract. Mech.*, vol. 74, pp. 1255–1273, 2007.
23. G. C. Sih and E. P. Chen, Cracks in Composite Materials, in G. C. Sih (ed.), *Mechanics of Fracture*, Martinus Nijhoff, The Hague, 1981.
24. Y. Murakami, S. Aoki, N. Hasebe, Y. Itoh, H. Miyata, N. Miyazaki, H. Terada, K. Tohgo, M. Toya, and R. Yuuki, *Stress Intensity Factors Handbook*, Pergamon Press, Oxford, New York, Beijing, Frankfurt, 1987.